Proceedings of the 20th International Conference on Soil Mechanics and Geotechnical Engineering– Rahman and Jaksa (Eds)

Landslide initiation in small-scale sandy and clayey slopes exposed to artificial rain

Initiation aux glissements de terrain dans de petites pentes sableuses et argileuses exposées à la pluie artificielle

Josip Peranić, Vedran Jagodnik, Nina Čeh, Sara Pajalić, Petra Jagodnik & Željko Arbanas
Faculty of Civil Engineering, University of Rijeka, 51000 Rijeka, Croatia, josip.peranic@gradri.uniri.hr

ABSTRACT: Physical modelling of landslides using scaled landslide models behaviour began in 1970s in Japan on scaled natural slope models. The laboratory experiments of landslide behaviour in a scaled physical model (flume or flume test) started in 1980s and 1990s in Canada, Japan and Australia under 1g conditions. The main purpose of the landslide physical modelling in the last 25 years was research of initiation, motion and accumulation of fast flow like landslides caused by infiltration of water in a slope. In this paper the results obtained in landslide initiation test of a sandy and clayey slopes at different slope angles exposed to artificial rain by rainfall simulator are presented. The results of landslide development are monitored by observation of volumetric water content, matric suction and pore water pressure, as well as by monitoring of surface displacements and the displacements inside the sliding mass. The main observations from the results of provided tests related to initiation and development of the observed instabilities of sandy and clayey slopes are given.

RÉSUMÉ : La modélisation physique des glissements de terrain à l'aide de modèles de comportement de glissement de terrain à l'échelle a commencé dans les années 1970 au Japon avec des modèles physiques de pente naturelle à l'échelle. Les expériences en laboratoire sur le comportement des glissements de terrain dans un modèle physique à l'échelle (test de canal ou de canal) ont commencé dans les années 1980 et 1990 au Canada, au Japon et en Australie dans des conditions de 1g. Le principal objectif de la modélisation physique des glissements de terrain au cours des 25 dernières années était la recherche sur l'initiation, le mouvement et l'accumulation d'écoulement rapide comme les glissements de terrain causés par l'infiltration d'eau dans une pente. Dans ce manuscrit, les résultats obtenus dans le test d'initiation de glissement de terrain sur des pentes sablonneuses et argileuses à différents angles de pente exposés à la pluie artificielle par un simulateur de pluie sont présentés. Les résultats du développement des glissements de terrain sont surveillés par l'observation de la teneur en eau volumétrique, de l'aspiration matricielle et de la pression interstitielle de l'eau, ainsi que par la surveillance du déplacement de surface et du déplacement à l'intérieur de la masse glissante. Les principales observations dans les résultats des tests fournis liés à l'initiation et au développement des instabilités observées des pentes sableuses et argileuses sont décrites.

KEYWORDS: physical modelling, small-scale slope, landslide, monitoring, artificial rain.

1 INTRODUCTION

Landslides are hazardous motions of a mass of rock, earth or debris down the slope (Cruden, 1991) that threaten vulnerable human settlements in mountains, cities, riverbanks, coasts and islands. An increase in the frequency and/or intensity of heavy rainfall, and a shift in the location and periodicity of these rainfalls due to changing climate can significantly increase the risk of landslides in some landslide-prone areas. Developments in mountainous and coastal areas, including the construction of roads and railways, expansion of urban areas and deforestation due to population growth and migration, increase exposure to the landslide hazard. Although not frequent, strong earthquakes have the potential to trigger rapid landslides with long runout distances. The combined effects of both triggering factors can lead to greater impacts from catastrophic landslides such as debris flows, rock falls and mega slides.

Combined efforts from scientists, engineers and all others included in landslide risk reduction resulted in significant development of landslide science in different fields: from landslide identification, mapping and investigation; identification of landslide susceptibility, hazard and risk; soil and rock testing; landslide modelling and simulation to landslide monitoring, mitigation and remediation. Research of landslide initiation represents the basis for understanding landslide processes as well as *conditio sine qua non* in implementation applicative studies related to landslide susceptibility, hazard and risk; landslide prediction and early warning as well as landslide prevention and remediation. Although the phenomenological approach can be applied, knowing only basic soil or rock mass parameters, in landslide trigger analyses, complex models of soil behaviour require more detailed knowledge on failure processes.

Modelling of landslide initiation for a long time was based only on numerical modelling techniques using soil strength and deformability parameters obtained from soil laboratory testing in direct shear apparatus, triaxial apparatus and ring shear apparatus. Despite the technology advancement, obstacles and limitations related to the sample size, sample disturbance, shear strain before the failure, effective stress measurements, drop in strength to the residual values, etc. still exists. For these reasons, physical modelling of landslide behaviour using small-scale models was introduced as a solution in different landslide researches.

Physical modelling of landslide by analysing small scale landslide models behaviour started in 1970s and 1980s in Japan (Oka 1972; Kutara and Ishizuka 1982; Yagi et al. 1985; Yamaguchi et al. 1989) on natural slopes exposed to artificial rainfall. The laboratory experiments of landslide behaviour in a scaled physical model (also called flume or flume test) started in 1980s and 1990s in Canada (Hungr and Morgenstern, 1984), Japan (Yagi et al., 1985) and Australia (Eckersley, 1990) under 1g conditions. On the other hand, geotechnical centrifuge was successfully adopted for small scale landslide modelling under increased acceleration (*n* times the gravity) (e.g. Kimura 1991; Take et al. 2004; Ling et al. 2009). This paper discusses small scale landslide modelling in 1g loading conditions.

After initial experiences with field and laboratory researches, the small-scale landslide modelling has found a wide application around the world in different aspects of landslide investigations, analysing different types of landslides (e.g. flows, slides, falls and toppling) as well as different types of materials (rock mass, sandy, silty and clayey materials) and landslide movements. The main task of landslide physical modelling was research of initiation, motion and accumulation of fast flow-like slides

caused by infiltration of surface water in a slope and fluidification. Small-scale landslide physical modelling was also oriented to the second most important triggering factor, i.e. earthquakes after 2005 (Hong et al. 2005; Wartman et al. 2005; Lin and Wang 2006), although the physical models in slope stability analyses were used much earlier (Clough and Pirtz 1956; Seed and Clough 1963; Goodman and Seed 1965).

Although the small-scale landslide physical models, modern monitoring techniques and different monitoring equipment enable good insight into initiation and development of modelled landslide, crucial issue is to establish relationship between small-scale, brief, idealized and by artificial boundary restricted model with the complex natural landslide process (Iverson, 2015). This relationship is known as scaling or scaling law, and plays a crucial role in small-scale model designing and interpretation of results. Successful scaling (of material parameters, model dimensions, boundary conditions, rainfall intensity and shaking parameters as triggering factors, measured movements, velocities and accelerations etc.) is a necessary precondition for realization of successful small-scale landslide modelling.

At the Faculty of Civil Engineering, University of Rijeka, Croatia, the research Project "Physical modelling of landslide remediation constructions' behaviour under static and seismic actions", funded by Croatian Science Foundation, started in October 2018. The main objective of the Project is modelling and analysing behaviour of landslide remedial measures in physical models of scaled landslides under static and seismic conditions (Arbanas et al., 2019). This paper presents the results of landslide initiation tests of sandy and clayey scaled slopes built with different inclinations and subjected to artificial rainfall. Landslide development was monitored by observing surface displacements using *structure-from-motion* (SfM) photogrammetry, terrestrial laser scanner (TLS) and a pair of high-speed cameras, and by observing landslide movements within the modelled displaced mass using accelerometers. Pore water pressure and soil moisture sensors were used to observe the hydraulic response of a slope. While the observed landslide movements are still being analysed, this paper presents the observations of landslide movements and the measurements of pore water pressures and water content within the slope. The differences in landslide initiation in sandy and clayey slopes are highlighted.

2 MATERIALS AND METHODS

The physical model of a scaled slope was designed to enable initiation of a landslide caused by controlled artificial rainfall and equipped with adequate photogrammetric equipment and complex sensor network with ability to measure displacements, soil moisture and pore water pressures within a slope (Figure 1) (Arbanas et al., 2020; Jagodnik et al., 2021). Dimensions of the flume are 1.0 m (width) x 2.3 m (length) x 0.5 m (height). The maximum depth of a soil material in the slope was adopted to be 30 cm. Flume slope inclination can be adjusted from 20° to 45°. To prevent possible sliding of the soil mass at the contact with the flume base, the geogrid mesh is fixed to the flume base to increase friction. The series of tests described in this paper were carried out on slope inclinations of 30° and 35° degrees with two different types of soil as slope material.

2.1 *Soil Material Properties*

To ensure the homogeneity of the soil material in the slope, two relatively simple materials were chosen to play the role of materials characteristic for slopes in Croatia. The properties of the materials are given in Table 1 and Figure 2. The fine grained (0 – 0.1 mm) Drava River sand was chosen as the base material

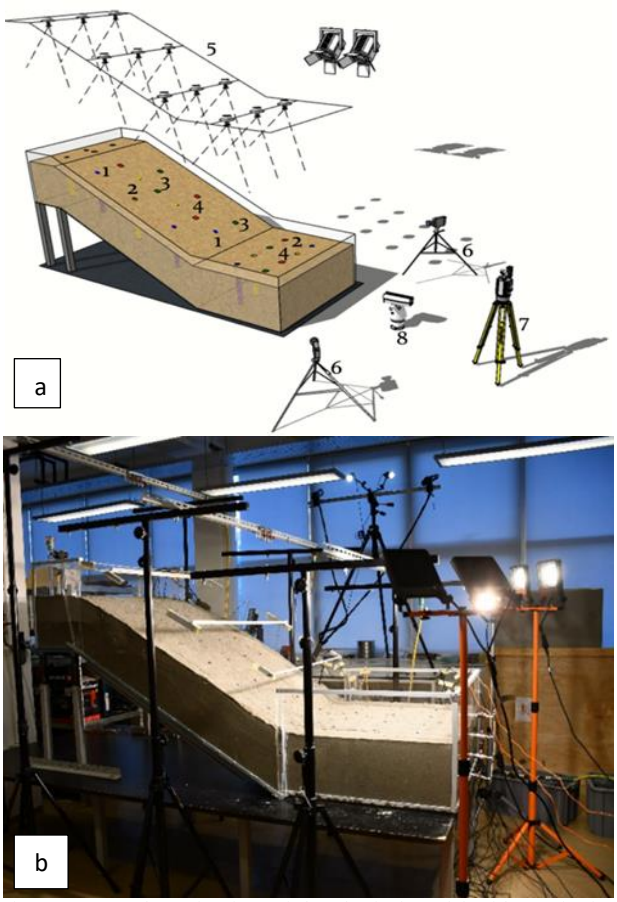

Figure 1. (a) Schematic view of the physical model with monitoring equipment: 1-tensiometers, 2-pore pressure transducers, 3-strain gauges, 4-accelerometers, 5-rainfall simulator (sprinkler system), 6-high speed cameras, 7-terrestrial laser scanner (TLS), 8-infrared camera; (b) Photo of the physical model (Arbanas et al., 2020; Jagodnik et al., 2021).

for the representation of the cohesionless slopes. Another material is a mixture of the base material with 10% by mass of industrial kaolin. Kaolin is chosen as clay with low plasticity and a relatively well graded grain size distribution curve and is not too sensitive to changes in water content. A mass of 10 % of kaolin was selected after a series of direct shear tests carried out on various sand-kaolin mixtures: it was noticed that the sand mixture with 10% of mass of kaolin clearly exhibited the behaviour of fine-grained, cohesive materials with stable cohesion. For this reason, the mixture of sand with 10% by mass of kaolin was used to represent cohesive slopes.

Friction angle and cohesion were determined in a direct shear apparatus at the same relative density of 50% and at low normal stresses similar to those in the slope model. Hydraulic conductivity was determined at same conditions as in the slope model, using the falling head test in an oedometer. The grain size distribution curves of the selected materials are presented in Figure 2, while Table 1 presents the basic physical properties and initial conditions at the start of the tests.

The previously described materials were installed in the flume in 5 layers, each 6 cm thick, up to a total height of 30 cm. Prepared sandy material with a water content of w=2% was installed using the under-compaction method (Ladd, 1978). Each layer was compacted using the manual compactor to the medium dense conditions of relative density $D_r = 50\%$. Before placing the next layer, the surface of the previous layer was raked and sprayed with a small amount of water to maintain the initial moisture content and achieve good contact between the particles of the two layers. In order to achieve homogeneity of the material in the slope and relatively uniform conditions in the built-up material,

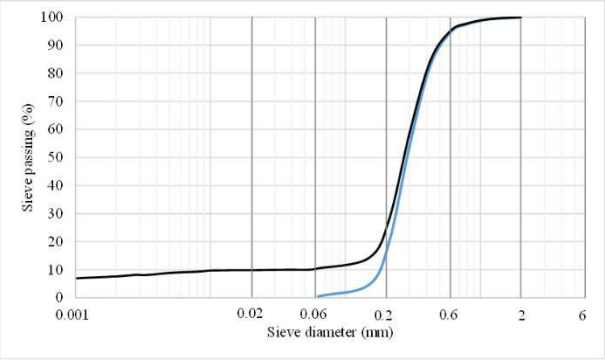

Figure 2. Grain size distribution curves of the Drava River sand (blue) and sand-kaolin mixture with 10% of mass of kaolin (black).

Table 1. Basic physical properties of the Drava River sand and sand-kaolin mixture with 10% of mass of kaolin built-in the model and initial conditions at the start of the tests.

Parameter	*Symbol*	*Sand*	*Sand-kaolin mixture*
Specific gravity	G_s	2.70	2.69
Dry density	ρ_d (g/cm^3)	1.52	1.43
Total density	ρ_t (g/cm^3)	1.55	1.50
Effective particle size	D_{10} (mm)	0.19	0.038
	D_{60} (mm)	0.37	0.31
Uniformity coefficient	c_u	1.947	8.16
Minimum void ratio	e_{min}	0.641	0.647
Maximum void ratio	e_{max}	0.911	1.121
Hydraulic conductivity	k_s (m/s)	1E-05	6.78E-06
Friction angle	ϕ (°)	34.9	31.3
Cohesion	c (kN/m^2)	0	3.9
Initial porosity	n_i	0.44	0.469
Initial void ratio	e_i	0.78	0.884
Initial relative density	Dr_i	0.5	0.5
Initial water content	w_i (%)	2	5

the model was built up in three segments – lower (L), middle (M) and upper (H) parts, building up the material from the foot to the top of the slope.

2.2 *Rainfall simulator*

One of the main difficulties in physical models simulating landslide initiation and motion caused by rainfall infiltration is to fully control the intensities of artificial rainfall applied to small-scale models. Rainfall simulators are widely used tools to study hydrological processes such as interaction of rainfall with soil, soil erosion, surface runoff and infiltration (Lora et al., 2016). Although it was possible to use some of the already developed rainfall simulators (Iserloh et al., 2013, 2012; Lora et al., 2016), a new rainfall simulator was constructed as part of the Project due to the lack of standard solutions. The rainfall simulator consists of three sprinkler branches, each equipped with four different axial-flow full-cone nozzles with a spray angle of 45° or 60°. Each branch has been placed at such a height that the water can reach the edges of the plexiglass sides without creating too much water on the edges or water coming out of the model. This solution covers a wide range of rainfall intensities, from less than 30 l/h/m^2 to more than 140 l/h/m^2 at a reference pressure of 2 bar. A wide range of rainfall intensities and the possibility to change the location of rainfall by opening or closing valves on each of the branches allows the modelling of different rainfall patterns and different rainfall intensities applied to the slope model (Arbanas et al., 2020).

2.3 *Monitoring equipment*

By definition, a landslide is characterised by a movement down the slope (Cruden, 1991), and observation of the movement distribution along a slope during the sliding process is one of the most important data for landslide analysis (Mihalić Arbanas and Arbanas, 2015). The monitoring system established in a physical model follows the principles used in the observation of real landslides and consists of a geodetic monitoring system and a geotechnical monitoring system. The geodetic monitoring system is based on innovative photogrammetric equipment for multi-temporal landslide analysis (Zanutta et al., 2006) of image sequences obtained by a pair of high-speed stereo cameras (Feng et al., 2016). Terrestrial laser scanning and *Structure-from-Motion* (SfM) photogrammetry surveys enable the surface of the slope model to be determined in pre- and post-slide phases (Bitelli et al., 2004). The geotechnical monitoring system comprises of a complex network of miniature sensors equivalent to the geotechnical monitoring devices used in the field (Wieczorek and Snyder, 2009). All sensors used in the tests are constantly connected to data loggers for continuous data collection during the time of the test. A detailed description of the equipment used in the geotechnical monitoring system is described in Pajalić et al. (2021).

3 TESTING RESULTS

After installing the soil in the slope model and installing monitoring equipment within the slope, the slope models were exposed to artificial rainfall from three nozzles, one nozzle in each part of the slope – upper, middle and lower part. Four tests were conducted and the basic data on the tests are given in Table 2. The course of the test developments is shown in Figure 3.

The results of four tests are presented in the following text: clean sandy material was used in Tests 1 and 2, while the mixture of sand with 10% of mass of kaolin was used in Tests 3 and 4, respectively. Both materials were built in slopes with inclination of 30° and 35°. Sandy materials were installed into the model at initial water content of 2%, while the sand-kaolin mixture was installed at initial water content of 5%. The installation of the material at the targeted initial water contents ensured the same initial densities and a direct comparison of the results of models built from the same material. The higher initial water content for the sand-kaolin mixture was necessary for effective compaction, as previously determined by the Proctor test. The initial water content could not be maintained during model construction; model construction extends over several days and evaporation and internal redistribution of water content are the reasons for the non-uniform water content distribution in a model at the start of the tests.

The slopes were exposed to different rainfall intensities: rainfall in the sandy slopes had intensities of 66 and 73 mm/h, while the slopes built of sand-kaolin mixture had intensities of 28 and 31 mm/h. The selection of rainfall intensities was based on infiltration conditions and the main requirement was that all the water at the point of contact on the model surface is infiltrated without forming surface runoff. The applied intensities were at the upper precipitation values that can be infiltrated in a soil.

After the initial establishment of a constant rainfall intensity and a stable infiltration process, the models were exposed to

Table 2. The basic data about conducted tests.

Test No.	*Material*	*Slope Angle (°)*	*Rainfall Intensity (mm/h)*	*Time to Initiation (min)*
Test 1	sand	30	66/122	126
Test 2	sand	35	73/55	62
Test 3	sand-kaolin	30	28	11
Test 4	sand-kaolin	35	31	24

rainfall at the constant intensities until the slope failed or until the end of the test. The end of the test was declared when further retrogressive sliding was no longer possible. In both tests which were conducted on sandy slopes, the failure mechanism was the same. The slope remained stable for a long time until the ground water level reached the slope surface in the foot of the slope and consequently caused a decrease in soil shear strength, sliding and further retrogressive landslide development towards the top of the slope. Tests were continued until the retrogressive slides reached the top of the slope (Figure 4a, c). The time from the rainfall start to the first signs of instability in the slope foot was relatively long (126 and 62 minutes), while the retrogressive development to the top of the slope occurred in the following 15 to 30 minutes.

In both tests conducted on slopes with sand-kaolin mixture, the failure mechanism was the same, but completely different from that observed in sandy slopes. Although the rainfall intensities were significantly lower than the intensities on sandy slopes, the first signs (cracks) of sliding appeared relatively quickly after the rainfall began (11 and 22 minutes). After appearance of the first cracks, the further retrogressive landslide development occurred to the top of the slope. This development was without significant movements in the slope; just new tension cracks were opening. The new stage occurred at the moment when the ground water level reached the slope surface in the middle part of the slope and forming small springs and surface flows (Figure 4b, d). At this moment, the joint mechanism of sliding and surface erosion started with a relatively fast retrogressive instability development up the top of the slope.

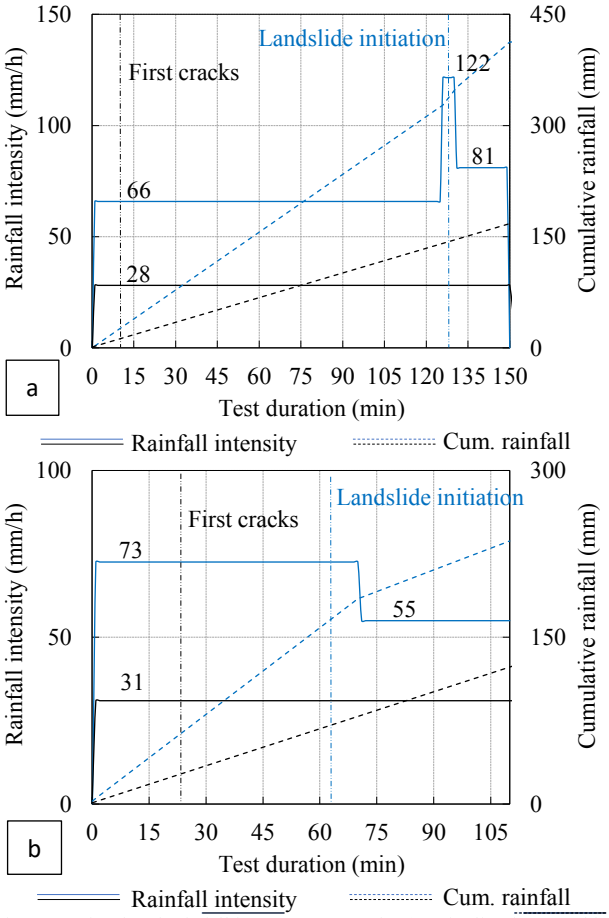

Figure 3. Simulated rainfall in: a) Tests 1 and 3 (30° inclination), and b) Tests 2 and 4 (35° inclination) on clean sand (blue) and mixture of sand with 10% of kaolin (black).

Figure 4. Photos of instabilities in small-scale slope model. (a) Sandy slope, 30° inclination, (b) Sand-kaoline mixture slope, 30° inclination, (c) Sandy slope, 35° inclination, (d) Sand-kaoline mixture slope, 35° inclination.

The described superficial signs of sliding initiations as well as the causes for their occurrence can be explained very well from the results of the continuous volumetric water content monitoring (Figure 5 and 6). Sensors measuring volumetric water content were installed at four different depths (6, 12, 18 and 24 cm below the slope surface) in the lower (L), middle (M) and upper (H) parts of the slope (Figure 5 and 6). The changes in volumetric water content in the different parts of the slope indicate the progress of the infiltration process until saturation of the soil and the formation of a ground water level; knowledge of this process allows a better understanding of sliding initiation.

By analysing the results presented, the processes in sand and sand-kaolin mixture slopes could be explained as follows. In the sandy slope, with relatively high hydraulic conductivity, the volumetric water content increases due to infiltration until saturation in the deepest part of the slope, forming the water table. As it becomes established, a flow down the slope begins, causing a rapid rise in the groundwater level in the lower part of the slope. This leads to a decrease in the soil shear strength with complete loss of matric suction, failure and further retrogressive landslide development to the top of the slope. For slopes made of sand-kaolin mixture, with significantly lower hydraulic conductivity, the process of saturation occurs first in the surface layer of the slope. This causes an increase in the weight of the surface layers and consequential cracking and shallow instabilities in the middle part of the slope without significant movements. The opening of the cracks allows water to penetrate deeper layers and formation of separated saturated zones in the slope, but the matric suction remains maintained in most of the slope. In some isolated local zones, near existing cracks, the ground water level forms and rises, causing flow with water coming out to the surface in the form of springs and surface flows, which in turn causes surface erosion. The water table forms only in the lowest part of the slope, while instabilities and erosion processes reach the top of the slope with a gradual loss of matric suction in the surface layers of the slope.

4 CONCLUSIONS

This paper presents the results of landslide initiation in small-scale slopes exposed to artificial rainfall. The results of four test conducted on two types of materials at different slope angles are presented. The observed failure mechanisms are described and

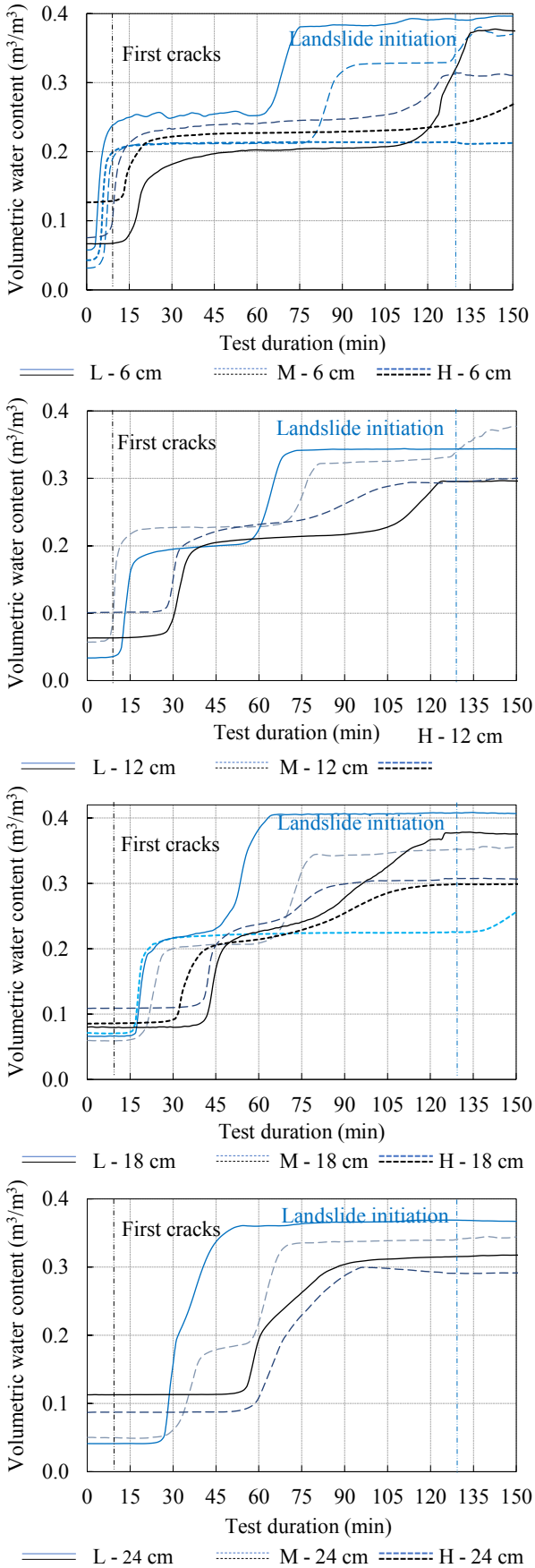

Figure 5. Volumetric water content measurements in Tests 1 and 3 (30° inclination) on clean sand (blue) and mixture of sand with 10% of kaolin (black) in upper (H), middle (M), and lower (L) profiles.

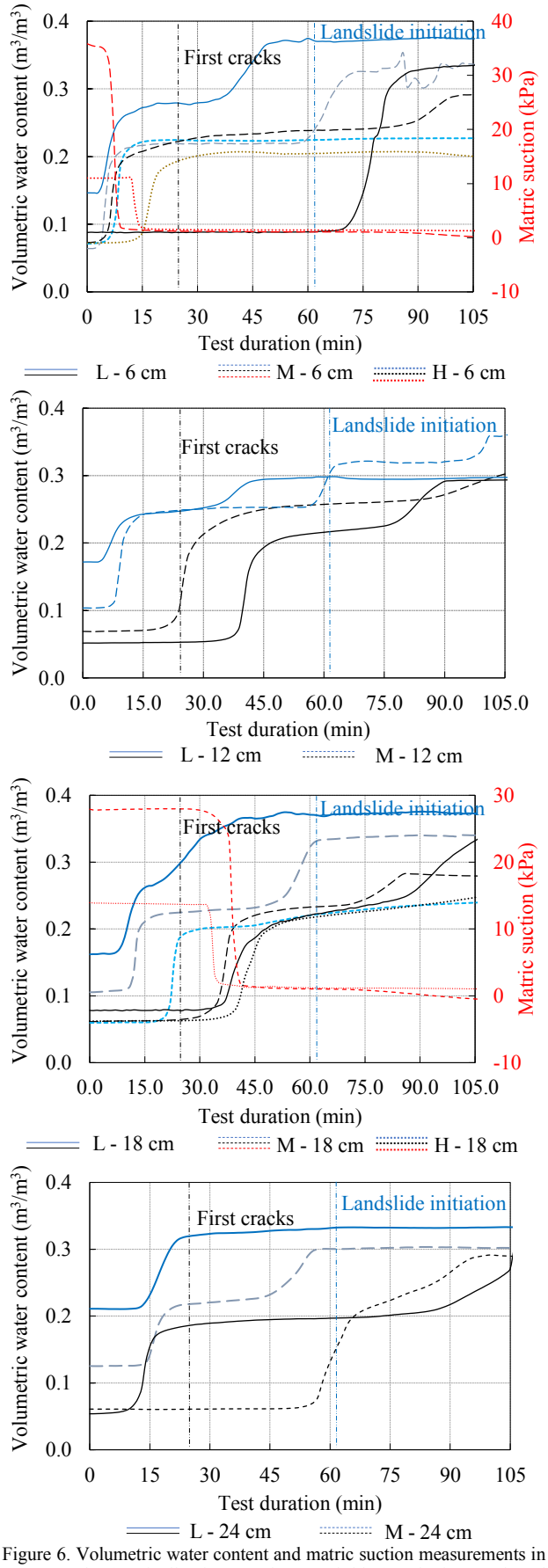

Figure 6. Volumetric water content and matric suction measurements in Tests 2 and 4 (35° inclination) on clean sand (blue) and mixture of sand with 10% of kaolin (black) in upper (H), middle (M), and lower (L) profiles.

explained, as well as the infiltration process based on the results of volumetric water content measurements. The results presented are the basis for the numerical analyses that will improve the insight into the processes and initiation of landslides in small-scale slope models.

Besides the monitoring results presented in this paper, several additional measurements have been carried out and are still being analysed. The results obtained by geodetic monitoring and the observations of surface movements should complete the analyses carried out, while the analyses of changes in matric suction, which are only briefly described in this paper, will play an important role in fully explaining the process of landslide initiation.

5 ACKNOWLEDGEMENTS

This research was funded by Croatian Science Foundation under the Project IP-2018-1503 Physical modelling of landslide remediation constructions behaviour under static and seismic actions (ModLandRemSS). The part of the laboratory equipment used for laboratory testing was provided in the frame of the Project Research Infrastructure for Campus-based Laboratories at the University of Rijeka, co-funded in a part by the Ministry of Science, Education, and Sports of the Republic of Croatia and the European Regional Development Fund (ERDF). These supports are gratefully acknowledged.

6 REFERENCES

Arbanas, Ž., Jagodnik, V., Peranić, J., Pajalić, S., Prodan, M.V., Čeh, N., 2020. Physical Model of Rainfall Induced Landslide in Flume Test: Preliminary Results, in: Proceedings of Europen Conference of Physical Modeling in Geotechnics. Presented at the 4th European Conference on Physical Modellining in Geotechnics, p. 8.

Arbanas, Ž., Pajalić, S., Jagodnik, V., Peranić, J., Vivoda Prodan, M., Đomlija, P., Dugonjić Jovančević, S., 2019. Development of physical model of landslide remedial constructions' behaviour, in: Proceedings of the 4th Regional Symposium on Landslides in the Adriatic - Balkan Region. Društvo za geotehniku u Bosni i Hercegovini, pp. 103–108. https://doi.org/10.35123/ReSy LAB_2019_17

Bitelli, G., Dubbini, M., Zanutta, A., 2004. Terrestrial laser scanning and digital photogrammetry techniques to monitor landslide bodies, in: International Archives of Photogrammetry, Remote Sensing and Spatial Information Sciences. Presented at the XXth ISPRS Congress: Geo-Imagery Bridging Continents, Istanbul, Turkey, pp. 246–251.

Clough, R.W., Pirtz, D., 1956. Earthquake Resistance of Rock-Fill Dams. Transactions of the American Society of Civil Engineers 123, 792–810.

Cruden, D.M., 1991. A simple definition of a landslide. Bulletin of the International Association of Engineering Geology 43, 27–29. https://doi.org/10.1007/BF02590167

Eckersley, D., 1990. Instrumented laboratory flowslides. Géotechnique 40, 489–502. https://doi.org/10.1680/geot.1990.40.3.489

Feng, T., Mi, H., Scaioni, M., Qiao, G., Lu, P., Wang, W., Tong, X., Li, R., 2016. Measurement of Surface Changes in a Scaled-Down Landslide Model Using High-Speed Stereo Image Sequences. Photogrammetric Engineering & Remote Sensing 82, 547–557. https://doi.org/10.1016/S0099-1112(16)82061-3

Goodman, R.E., Seed, H.B., 1965. Displacement of Slopes in Cohesionless Materials During Earthquakes (No. H21). Department of Civil Engineering, Institute of Transportation and Traffic ….

Hong, Y.-S., Chen, R.-H., Wu, C.-S., Chen, J.-R., 2005. Shaking table tests and stability analysis of steep nailed slopes. Canadian Geotechnical Journal 42, 1264–1279. https://doi.org/10.1139/t05-055

Hungr, O., Morgenstern, N.R., 1984. Experiments on the flow behaviour of granular materials at high velocity in an open channel. Geotechnique 34, 9.

Iserloh, T., Fister, W., Seeger, M., Willger, H., Ries, J.B., 2012. A small portable rainfall simulator for reproducible experiments on soil erosion. Soil and Tillage Research 124, 131–137. https://doi.org/10.1016/j.still.2012.05.016

Iserloh, T., Ries, J.B., Arnáez, J., Boix-Fayos, C., Butzen, V., Cerdà, A., Echeverría, M.T., Fernández-Gálvez, J., Fister, W., Geißler, C., Gómez, J.A., Gómez-Macpherson, H., Kuhn, N.J., Lázaro, R., León, F.J., Martínez-Mena, M., Martínez-Murillo, J.F., Marzen, M., Mingorance, M.D., Ortigosa, L., Peters, P., Regüés, D., Ruiz-Sinoga, J.D., Scholten, T., Seeger, M., Solé-Benet, A., Wengel, R., Wirtz, S., 2013. European small portable rainfall simulators: A comparison of rainfall characteristics. CATENA 110, 100–112. https://doi.org/10.1016/j.catena.2013.05.013

Iverson, R.M., 2015. Scaling and design of landslide and debris-flow experiments. Geomorphology 244, 9–20. https://doi.org/10.1016/j.geomorph.2015.02.033

Jagodnik, V., Peranić, J., Arbanas, Ž., 2021. Mechanism of Landslide Initiation in Small-Scale Sandy Slope Triggered by an Artificial Rain, in: Arbanas, Ž., Bobrowsky, P.T., Konagai, K., Sassa, K., Takara, K. (Eds.), Understanding and Reducing Landslide Disaster Risk: Volume 6 Specific Topics in Landslide Science and Applications, Springer International Publishing, Cham, pp. 177–184. https://doi.org/10.1007/978-3-030-60713-5_19

Kimura, T., 1991. Failure of fills due to rain fall, in: Centrifuge. Balkema, pp. 509–516.

Kutara, K., Ishizuka, H., 1982. Seepage flow in the embankment and stability of slope during rain (in Japanese). Tsuchi-to-kiso, Paper No 1330.

Ladd, R.S., 1978. Preparing Test Specimens Using Undercompaction. GTJ 1, 16–23. https://doi.org/10.1520/GTJ10364J

Lin, M.-L., Wang, K.-L., 2006. Seismic slope behavior in a large-scale shaking table model test. Engineering Geology 86, 118–133. https://doi.org/10.1016/j.enggeo.2006.02.011

Ling, H.I., Wu, M.-H., Leshchinsky, D., Leshchinsky, B., 2009. Centrifuge Modeling of Slope Instability. J. Geotech. Geoenviron. Eng. 135, 758–767. https://doi.org/10.1061/(ASCE)GT.1943-5606.0000024

Lora, M., Camporese, M., Salandin, P., 2016. Design and performance of a nozzle-type rainfall simulator for landslide triggering experiments. CATENA 140, 77–89. https://doi.org/10.1016/j.catena.2016.01.018

Mihalić Arbanas, S., Arbanas, Ž., 2015. Landslides: A Guide to Researching Landslide Phenomena and Processes. Handbook of Research on Advancements in Environmental Engineering 474–510. https://doi.org/10.4018/978-1-4666-7336-6.ch017

Oka, H., 1972. Impacts by the "artificial landslide": re-examine the rage of nature (in Japanese). Kagaku Asahi 32, 152–153.

Pajalić, S., Peranić, J., Maksimović, Sandra, Čeh, N., Jagodnik, V., Arbanas, Ž., 2021. Monitoring and Data Analysis in Small-Scale Landslide Physical Model. Applied Sciences 28.

Seed, H.B., Clough, R.W., 1963. Earthquake Resistance of Sloping Core Dams. Journal of the Soil Mechanics and Foundations Division 89, 209–242.

Take, W.A., Bolton, M.D., Wong, P.C.P., Yeung, F.J., 2004. Evaluation of landslide triggering mechanisms in model fill slopes. Landslides 1, 173–184. https://doi.org/10.1007/s10346-004-0025-1

Wartman, J., Seed, R.B., Bray, J.D., 2005. Shaking Table Modeling of Seismically Induced Deformations in Slopes. Journal of Geotechnical and Geoenvironmental Engineering 131, 610–622. https://doi.org/10.1061/(ASCE)1090-0241(2005)131:5(610)

Wieczorek, G.F., Snyder, J.B., 2009. Monitoring slope movements, in: Geological Monitoring. Geological Society of America. https://doi.org/10.1130/2009.monitoring(11)

Yagi, N., Yatabe, R., Enoki, M., 1985. Laboratory and Field Experiments on Prediction Method of Occuring Time of Slope Failure due to Rainfall. Journal of Japan Landslide Society 22, 1-7_1. https://doi.org/10.3313/jls1964.22.2_1

Yamaguchi, I., Nishio, K., Kawabe, H., Shibano, H., Iida, C., 1989. Initiation and fluidization of an artificial landslide: Field experiment in Yui Shizuoka Prefecture, Japan (in Japanese). Shinrin Kosoku (Areal Survey) 158, 3–9.

Zanutta, A., Baldi, P., Bitelli, G., Cardinali, M., V, A., 2006. Qualitative and quantitative photogrammetric techniques for multi-temporal landslide analysis. Annals of Geophysics 49. https://doi.org/10.4401/ag-3117